Magnetic Field Triggering of Excess Power in Deuterated Palladium

Scott R. Chubb* and Dennis G. Letts**

ABSTRACT : This paper reports the observation of excess power produced from deuterated palladium co-deposited on a copper substrate; the power gain was triggered by a 90 degree rotation of the cathode with respect to an external magnetic field of approximately 500 gauss. A 90 degree cathode rotation using light water electrolyte did not produce excess power. A description of the Seebeck calorimeter used for the measurement is also provided, including the Seebeck calibration methods. A plausible theoretical basis for the excess power result is also discussed.

Introduction

Fleischmann, Pons and Hawkins claimed to observe excess power in heavy water electrolysis experiments in March 1989.[1] The power densities reported in these early experiments were commensurate with nuclear power densities and led to the controversial claim of room temperature nuclear fusion, or "cold fusion." There is now enough diverse experimental evidence to support the claims for excess power[2] and that the reactions appear to be nuclear in origin.[3,4]

From inception, the Fleischmann-Pons excess heat effect was difficult to reproduce; long periods of electrolysis were required to initiate excess power in deuterated palladium cathodes and many early experiments failed.[5]

In 1993, Bockris and his co-workers introduced the idea of an external triggering mechanism to initiate the excess heat effect; in their work, RF and a magnetic field were observed to be effective in triggering excess heat in a deuterated palladium cathode.[6] Independently, Cravens reported a similar result in a paper presented at ICCF4.[7] Over the years, single and dual lasers were also demonstrated to be effective in producing excess power from deuterated palladium cathodes, in conjunction with external magnetic fields.[8,9]

In the past 20 years, external magnetic fields have been applied to many Fleischmann-Pons electrolysis cells but virtually no effort has been made to measure separately the effect of a changing magnetic field on thermal power output. Theoretical support for this type of experiment has also been lacking. This paper attempts to remedy those deficiencies.

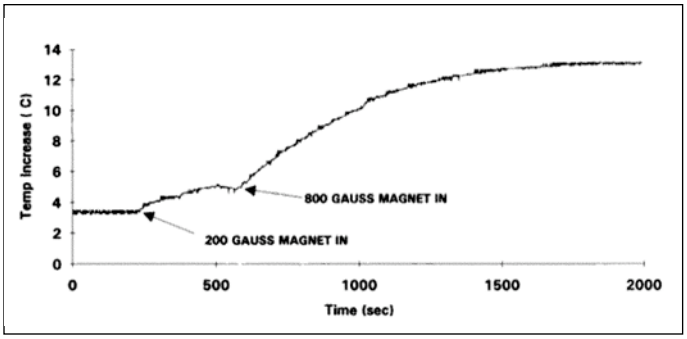

Figure 1. Magnetic fields of 200-800 gauss appear to trigger significant temperature increases during electrolysis of a deuterated palladium cathode.

1993 Magnetic Field Experiment

An early Fleischmann-Pons experiment performed by Letts and reported by Bockris produced an exothermic response to an imposed magnetic field[6]; the experiment was not well controlled but showed that a magnetic field of a few hundred gauss seemed to trigger a sudden and large cell temperature response, as shown in Figure 1.

This 1993 experiment shows that there may be a threshold for onset of the heat effect near 150-200 gauss and that the magnitude of the thermal response seems proportional to the magnetic field. No effort was made to perform careful calorimetry due to the preliminary nature of the experiment. Crude measurements indicated that a temperature increase of approximately 5°C required application of 1 watt of electrolysis power to the cell, implying that the 800 gauss magnet may have triggered approximately one watt of excess power.

2002 Magnetic Field Experiment

In 2002, Letts performed another magnetic field test with similar results but used better lab equipment and methods. Two small magnets were kept in constant thermal contact with the outside of a cylindrical glass vessel and rotated 90

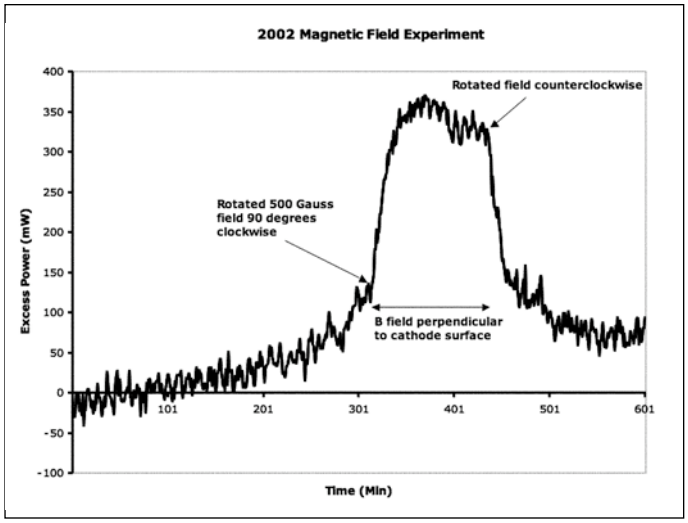

Figure 2. Rotating a magnetic field 90 degrees increased the thermal power output of a Fleischmann-Pons Pd/LiOD electrolysis cell.

degrees. When the palladium cathode was electrolyzed in LiOH, cell temperature did not increase. When LiOD was used as the electrolyte, cell temperature increased by about 1°C. When the magnets were put back in their original position, the excess power signal declined. During calibration, it was determined that a cell temperature increase of 1°C required the addition of approximately ¼ watt of electrolysis power to the cell. The result is shown in Figure 2.

Cell geometry is shown in Figure 3. When the magnetic field lines are across the face of the cathode, excess power is minimal or zero; when the magnetic field lines are perpendicular to the face of the cathode, excess power is observed.

2010 Magnetic Field Experiment

In 2010, Letts was motivated to test the magnetic field effect again using a Seebeck calorimeter designed and built at Lettslab in Austin, Texas. Five hundred gauss magnets were permanently built into the calorimeter, making it possible to change the cathode-magnetic field geometry by simply rotating the cathode electrode holder (Figures 3, 4).

The core of the Seebeck calorimeter is a piece of square borosilicate glass 45 mm wide, 150 mm long and 2 mm thick (Friederich & Dimmock, #BST45-200) with a square-to-round transition so that a screw-in Teflon lid can be used to seal the cell, as shown in Figure 4. Thermal electric converters 50 x 50 mm square were epoxied to the outside of the glass walls using Duralco 128 thermal epoxy from Cotronics Corp. Ten percent by weight of flexibilizer was added to the epoxy to avoid thermal expansion damage (Cotronics 105RF-1). Aluminum heat sinks were machined and epoxied to the cool side of the thermal electric converters using Duralco 128. A constant airflow was applied up the vertical axis of the Seebeck calorimeter from a brushless DC fan from Radio Shack. Figure 5 is an overview of the experiment.

The calorimeter provides a 1% level of thermal precision and has been tested from 0.25 watts to 25 watts. The calibration used for the 2010 magnetic field experiment is shown in Figure 6. The calibration was run using LiOH at 0.15 M; the cathode was a platinum foil 4 x 10 x 0.25 mm, the anode was a coil with an inside diameter of 12 mm. An immersion heater was used at 11 watts of constant power to keep the recombiners warm. The calorimeter reports 302 mV when electrolysis power is zero because of the immersion heater (Figure 6).

Experiment 690 was conducted in February 2010 to test the magnetic field effect on deuterated palladium using the Seebeck calorimeter. For the first time in 17 years, it was possible to test the magnetic trigger effect in a reliable calorimeter—the previous tests at Lettslab used isoperibolic calorimetry methods and were not suited to testing a magnetic trigger. The electrode assembly used for this test is shown in Figure 7. In

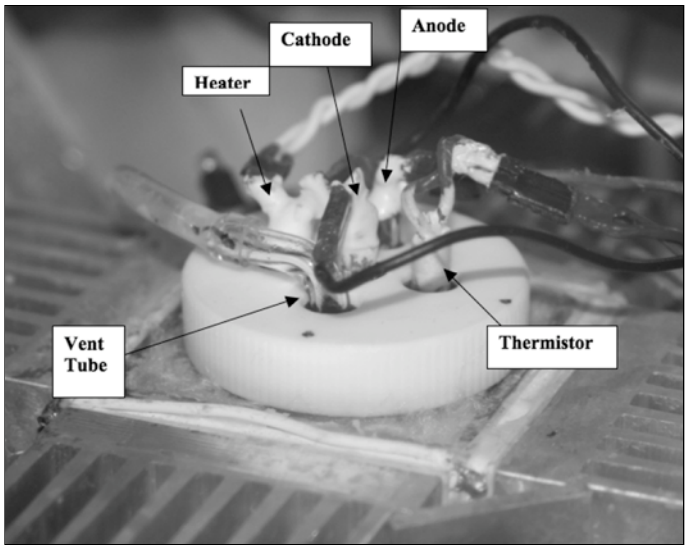

Figure 4. The Seebeck calorimeter's Teflon lid and pass-throughs.

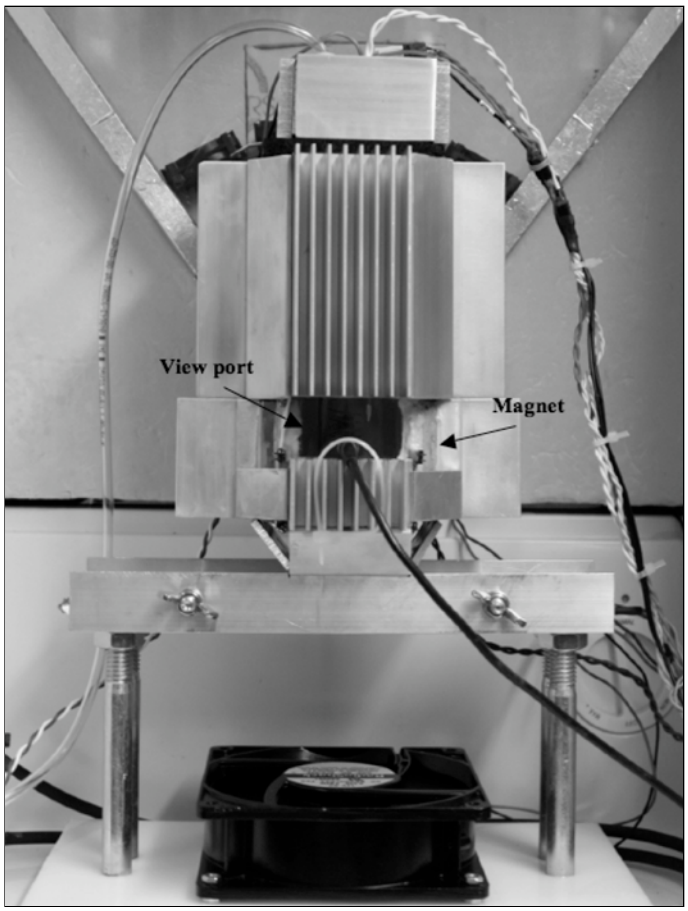

Figure 5. The Seebeck cell/calorimeter in a controlled enclosure to maintain ambient temperature at 25 ± 0.02°C.

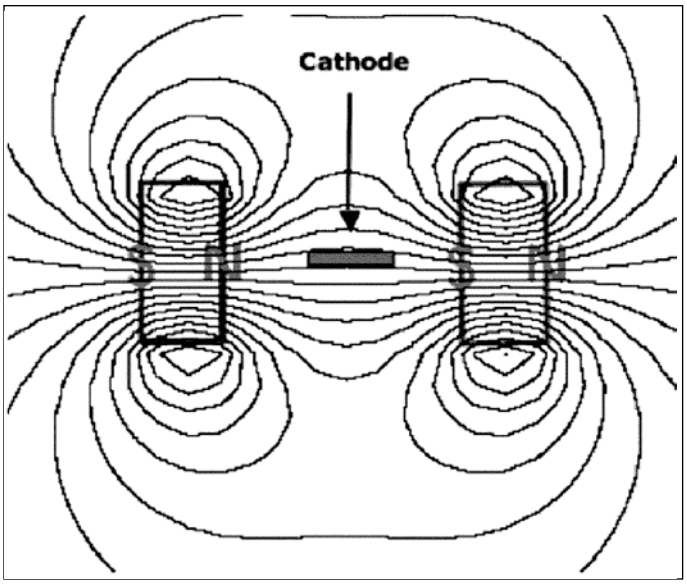

Figure 3. The cathode position with respect to field lines when excess power is not observed.

this experiment, the cathode was co-deposited with palladium in an electrolyte of 0.15M LiCl and 0.025M $PdCl_2$, which produced a modest amount of excess power. After excess power was established, the glass cathode holder shown in Figure 7 was rotated 45 degrees and then 90 degrees. Additional excess power gain was observed, as shown in Figure 8.

The overall thermal response of the cell was in excess of a 60% gain in thermal power output after rotation of the cathode to change the magnetic field direction by 90 degrees.

After the test in D_2O was made, another cathode was made identical to the cathode used to produce the result in Figure 8 but electrolyzed in an H_2O-based electrolyte. When the cathode was rotated 90 degrees in this test, there was a large disturbance to the cell but there was no lasting excess power, as shown in Figure 9.

A Post-Experiment Calibration Check

After completing the test in H_2O (Figure 9), the calorimeter was checked by stopping electrolysis and allowing the cell to equilibrate. Then a LiOH cell on the benchtop was electrolyzed with platinum electrodes at a constant current of 1 amp. This cell was run without recombiners and the produced hydrogen and oxygen gases were conducted into the calorimeter via a small rubber tube. The gases were bubbled up through the electrolyte and allowed to recombine on the recombiner pellets, shown in Figure 7. The immersion heater, also shown in Figure 7, was left on at 11 watts to keep the recombiners warm and functioning at 100% efficiency.

Under these conditions, if the Seebeck calorimeter was still in good calibration, it should report ~1.48 watts of excess power due to the hydrogen and oxygen recombining in the cell. The results of this post-experiment calibration check are shown in Figure 10.

The gas flow of hydrogen and oxygen was switched on at about point 25; the Seebeck responded quickly and its thermal output reached equilibrium around point 90. The average of the apparent excess power from recombination of gases from an external source was ~1.464 W. The expected value was 1.481 W if the experiment was conducted at 298.15 K. However, the experiment was conducted at approximately 323.15 K, making the expected value ~1.477 W.[10] This suggests that the calorimeter was and is in good calibration to an accuracy of 1.464/1.477 ~99%. At point 255 the gas flow was shut off and the calorimeter regained thermal equilibrium by point 400.

Potential Explanation of Impact of Magnetic Field Orientation on Excess Power

Overview

The series of experiments reported in this paper cover 17 years of experimental history and show a similar pattern for bulk palladium (Pd) and for co-deposited Pd. The effect was first observed under very poor calorimetric conditions, but the effect persisted even when tested with a good quality Seebeck calorimeter many years later. The key results observed in this study were:

- The Seebeck calorimeter reports excess power reliably.
- Co-deposition methods produced an average of 120 mW before cathode rotation.
- Rotating the cathode 90 degrees in D_2O increased excess power to 200 mW.
- Rotating the cathode 90 degrees in H_2O had no effect.

The most surprising (and potentially most interesting) of these results is the third one. Although the effect was not expected, it may have a logical and plausible theoretical explanation, based on the Ion Band State Theory (IBST) of low-energy nuclear reactions (LENR).[11] In the IBST, the Fleischmann-Pons excess heat effect results from a form of deuteron (d)+d→^{4}He nuclear fusion reaction, without high-energy particle emission, that can potentially be initiated when the interacting d's and the ^{4}He product occupy wave-like, ion band states (IBS's) similar to the kinds of wave-like (energy band) states that electrons occupy in ordinary metals. The theory is based on a generalization of the conventional theory of electronic structure, and charge and heat transport in solids associated with electron energy band states.

In the simplest situation, it is possible to understand how either through an internally generated electrical ($\vec{E}$) field that is induced as a result of the process of loading deuterium (D) atoms into Pd (as well as by co-depositing D and Pd onto a substrate) or by externally applying an $\vec{E}$-field, it is possible to trigger nuclear reactions. Because the underlying physics of the associated effect can be explained using the conventional

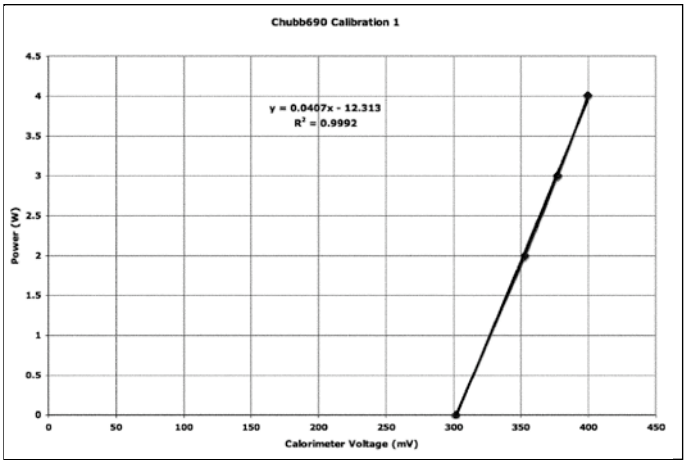

Figure 6. The calorimeter produces a linear calibration over the power range used for the experiment. A new calibration is performed before beginning a new experiment.

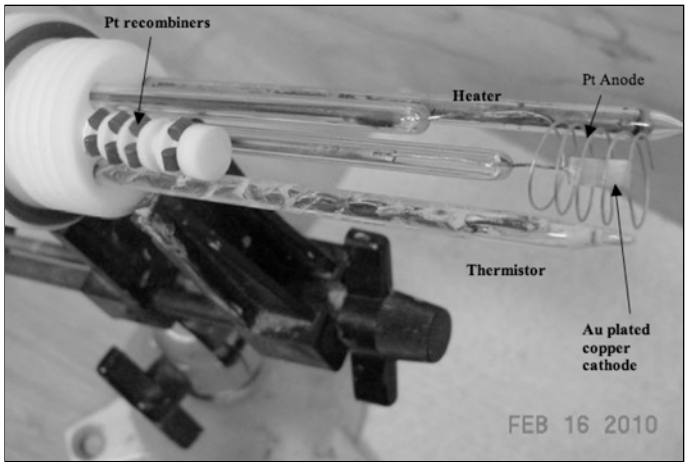

Figure 7. The 5 mm diameter sealed glass tubes. Hook up wire is 0.5 mm platinum wire spot welded to copper wire sealed inside the glass tubes.

theory of charge conduction in periodically ordered solids, it is also possible to understand how the triggering effect can be altered as a result of introducing an externally applied magnetic ($\vec{B}$) field. The concept is based on extending the well-known effects associated with the "semi-classical" picture that has been used to describe how electrons in energy band states are affected when such a field is introduced to a comparable situation in which ions occupy these kinds of states.

Within this context, it is possible to show that a coherent triggering mechanism is allowed to proceed as it would in the absence of an applied $\vec{B}$-field when the $\vec{B}$-field is parallel (or anti-parallel) to the $\vec{E}$-field. But when the $\vec{B}$- and $\vec{E}$-fields are perpendicular to each other, the triggering effect is blocked as a result of a kinematical constraint that prevents the current from inducing the necessary increase in momentum that is required for nuclear reaction to occur. The presence of the $\vec{B}$-field has two additional important effects: 1) It establishes a preferential orientation for creating nuclear reactions (in which the ^{4}He is created along paths that are perpendicular to $\vec{B}$); 2) It can induce a process that can help to remove ^{4}He from the solid in a manner that minimizes disruptions of the underlying periodic order, which is required for the reactions to occur.

These last two effects, as well as the triggering effect, are required in order to maintain periodic order for a sufficiently long time in a sufficiently large crystal. In fact, the generalization of conventional energy band theory that is the basis of IBST provides a framework for estimating the amount of time that is required for this to occur. Hence, it is possible to construct a self-consistent picture that quantifies how these various effects are related to each other and to other factors (most notably, the size of the crystal necessary to sustain the triggering effect). In order to quantify the resulting description and to provide a meaningful context for its application, it is necessary to provide some background material about the underlying framework of the theory.

In the following subsections, information is presented about the theory and its relevance (a) to existing information about excess power in cold fusion experiments and (b) in other contexts involving more conventional phenomena. Included are: an explanation about how the effects of an external magnetic field can establish a preferential orientation for creating nuclear reactions; general information about charge conduction, based on conventional energy band theory, and its generalization to situations involving finite-size crystals; explanation of a key coherent process (that forms the basis of both conventional energy band theory and its generalization) that can explain how to trigger nuclear reactions, in the simplest (order-preserving) situation; context for understanding the relevance and applicability of this process generally, where collisions and disorder are allowed to take place; introduction of modifications of the associated triggering process that result from the presence of an external magnetic field and, based on the associated analysis, an explanation of the reason that excess power occurs when the $\vec{B}$- and $\vec{E}$-fields are parallel or anti-parallel to each other and why excess power does not occur when these fields are perpendicular to each other; suggestions for new experiments for enhancing the production of excess power, based on the requirement that ^{4}He be eliminated from the crystal in an optimal (order-preserving) manner in the presence of $\vec{B}$ and $\vec{E}$ (and potentially other) fields.

Background on the Ion Band State Theory (IBST)

Evidence exists[12-15] that in certain situations, hydrogen and deuterium nuclei occupy "wave-like" ion band states (IBS's) in[15] and on the surfaces[12-14] of transition metals. For this reason, a physically plausible argument can be made that the starting point of the theory (that hydrogen and deuteri-

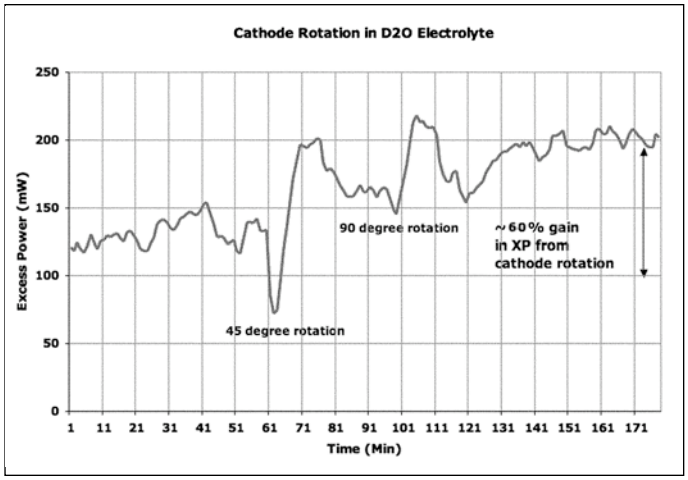

Figure 8. The cell produced ~120 mW of excess power before cathode rotation; at point 61 the cathode was rotated 45 degrees, then 90 degrees at point 101.

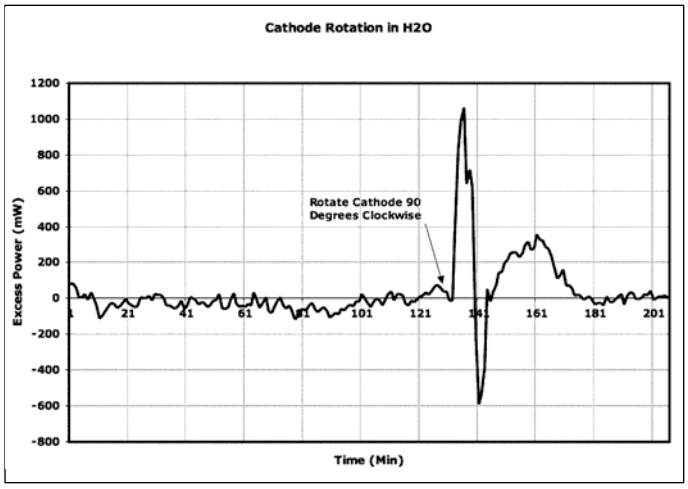

Figure 9. Rotating the cathode to change the direction of the magnetic field lines with respect to the cathode by 90 degrees has no lasting affect on thermal power output when the electrolyte is H_2O.

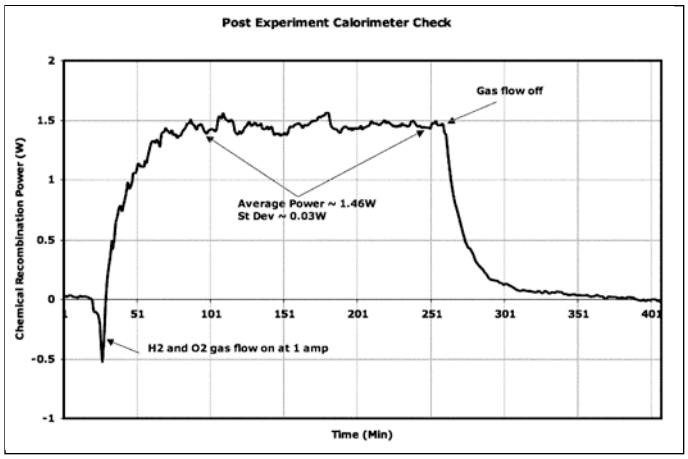

Figure 10. The calorimeter correctly measures the thermoneutral potential for hydrogen and oxygen recombination to an accuracy of ~99%.

um nuclei can occupy band states) makes sense. Over the years, in order to more fully understand the potential relationship between situations in which d's occupy IBS's and the possibility that nuclear reaction can occur, it has been necessary to generalize approximate ideas associated with the conventional energy band theory. That theory has been used to describe the behavior of electrons in infinitely-repeating, periodic crystal lattices to situations in which the lattices have finite extent.[11,16] A summary of key features of the IBST is provided in Chubb.[11] The underlying assumptions of the theory were presented many years ago.[17-19]

Through the theory, a number of key effects associated with the Fleischmann-Pons (FP) heat effect were predicted prior to their being observed experimentally. These included the following experimental observations: 1) ^{4}He is produced at levels that account for the large amounts of excess heat that FP observed[20,21]; 2) ^{4}He appears in an unanticipated location, outside heat-producing electrodes[20,21]; 3) There is an apparent requirement that for the effect to occur, "high-loading" ($x \rightarrow 1$ in PdD_x) is required[22,23]; 4) The effect occurs without the emission of any high-energy particles or radiation.[20,21,23]

The theory also predicts that the d+d→^{4}He reaction occurs in crystals (or portions of a crystal) that can have a characteristic dimension a that is as small as 1-2 nm. Details about the associated model become more rigorous in larger crystals, in which a (>~1μm). In the case of PdD, an even more rigorous picture is applicable. In particular, d's can occupy IBS's as a result of small fluctuations in loading $\delta <\sim 10^{-4}$ in $PdD_{1\pm\delta}$. When this occurs, each d that enters the lattice during the fluctuation effectively can split into many small ("wave-like") pieces, which are distributed throughout the lattice, leading to a situation in which small concentrations (~δ) of d's may interact in a nuclear fashion at many different locations. As a consequence, the charge, momentum and energy associated with each nuclear reaction become distributed between many locations, simultaneously, and each final state ^{4}He nucleus created through the process also occupies an IBS and is also split-up into many wave-like pieces.

The reason this occurs is fundamentally related to the underlying electronic structure. In PdD, the fluctuations involving $\delta <\sim 10^{-4}$ are associated with a highly-polarized, anti-bonding situation in which each electron that enters the solid with each D-nucleus effectively dissociates from it. As a consequence, the lowest energy acoustical phonons in finite crystals of PdD actually are not really phonons (because they result from vibrations that do not conserve charge); when they are produced, they create residual (positive) charge that results from the very different time-scales associated with the motions of the electron and D-nucleus for each D atom that is involved in the fluctuation.

In order to minimize energy in the limit of very small IBS concentration, the residual positive charge is required to be located near the octahedral sites associated with conventional loading. Opposed to the normal situation associated with conventional loading, in which each octahedral site is occupied by a single d, each d that occupies an IBS contributes a small (~1/10,000) fraction of a single d at each of these sites.

In order for reactions to proceed most effectively in this way, the theory requires that the most coherent, slowest reactions occur. These preserve approximate periodic order over a sufficiently large region, and the system energy (including the behavior of all of the potential excitations of the crystal) is minimized in regions where the reaction takes place. In this limit, residual ^{4}He that is created can only appear in wave-like, IBS's formed in the interior (bulk) regions of the crystal; when it becomes neutralized in the surface regions of the solid (or at the locations of lattice imperfections), heat is released through the neutralization process (leading to the generation of long wavelength phonons).

The theory also predicts an important relationship between the rate of nuclear reaction, R, the concentration, c_d, of d's that are initially in IBS's, and the concentration, $c_{^4\mathrm{He}}$, of ^{4}He nuclei that occupy IBS's after each reaction:

$$R \propto c_{\mathrm{d}}^2 \, c_{^4\mathrm{He}} \qquad (1)$$

The fact that R is proportional to $c_{^4\mathrm{He}}$ has significant consequences. It means that a form of "self-stimulation," in principle, can take place in which the presence of ^{4}He nuclei in IBS's can induce additional ^{4}He nuclei to occupy IBS's. This is implied by Equation 1 because it suggests that an increase in $c_{^4\mathrm{He}}$ should induce an increase in R, which in a situation involving a fixed volume should lead to an increase in $c_{^4\mathrm{He}}$.

The origin of this self-stimulation is associated with the fact that each ^{4}He nucleus is a boson. In analogy with stimulated emission of photons in lasers, "self-stimulated" creation of ^{4}He nuclei from fusion can take place in the FP excess heat effect when it occurs through IBS interaction. However, there is an important distinction: because each ^{4}He nucleus that is created is required to occupy an IBS, and approximate periodic order is necessary in order for any IBS to be occupied, any energy that is produced must be dissipated in such a way that periodic order is preserved in the region where IBS's are occupied. In practice, the most effective way for this to occur involves a situation in which heat from nuclear reactions is dissipated at the boundaries of the crystal (or near lattice imperfections).

But left unchecked, the self-stimulation process will increase R; this will induce phonon generation in internal regions, thereby inducing heat and disorder, when $c_{^4\mathrm{He}}$ is allowed to increase. Energy minimization arguments[24] imply that there is a size limitation associated with initiating the d+d→^{4}He reaction. Effectively, a minimal volume (~650 unit cells) in which the required periodic order is maintained is necessary. For this reason, accumulations of phonons (especially localized phonons) and heat disrupt the process and, as a consequence, if $c_{^4\mathrm{He}}$ increases beyond a critical value, the process will turn itself off.

This means that self-stimulated heat in internal regions not only destroys the reaction process, but the rate at which it is produced provides a rate-limiting step for the entire process of occupying (and/or instigating interactions involving) IBS's. For this reason, the most effective ways of producing excess heat through IBS interactions require that each ^{4}He nucleus that is produced not only occupy an IBS in the bulk (interior) regions but that it be expelled from the bulk into the surface regions and the off-gases.

In the generalization of conventional energy band theory to finite crystals, the occupation of energy bands and charge transport are intimately tied to conditions associated with net flux conservation.[11,16] The total fluxes of particles that are allowed to occupy band states between interior and exterior regions remain in balance so that their sum vanishes. It

is plausible that this fact is related to the observation that excess power is approximately proportional to the magnitude of the flux of D-atoms into the electrodes, in electrolytic experiments.[25]

A further required condition is that a selection rule known to apply in the free space d+d→^{4}He reaction (in which a γ ray is produced) must also apply in the FP excess heat form of the reaction. A requirement for the reaction to occur is that the initial (d+d) and final (^{4}He) states have vanishing spin. Although this selection rule is not absolutely required inside a solid, in the most coherent processes that have minimal coupling to the environment, this rule does apply. Because processes that maintain periodic order are required, this kind of minimal coupling to the environment is necessary.

How External Magnetic Fields Can Establish a Preferential Nuclear Reaction Orientation

The presence of an external magnetic field $\vec{B}$ always induces a precession of the spins of charged particles that interact with it, in directions normal to $\vec{B}$. The Bloch equations, which describe the time evolution of the expectation value of the components of the spin $<\vec{S}(t)>$, can be used to illustrate this effect. In vector form, these equations are given by the following:

$$\frac{\partial <\vec{S}(t)>}{\partial t} = \omega_L <\vec{S}(t)> \times \hat{B}\,, \qquad (2)$$

where $\hat{B} = \vec{B}/|\vec{B}|$ is a unit vector, pointing along the direction of $\vec{B}$, $\omega_L = \mu|\vec{B}|/\hbar$ is referred to as the (angular) Larmor frequency, associated with the particle (possessing magnetic moment μ) that interacts with $\vec{B}$. The solution of Equation 2 is:

$$<S(t)> = \hat{B} \times (<\vec{S}(0)> \times \hat{B})\cos(\omega_L t) \qquad (3)$$
$$+ \hat{B} \times <\vec{S}(0)> \sin(\omega_L t) + \hat{B}\hat{B} \bullet <\vec{S}(0)>\ .$$

From Equations 2 and 3, it follows that $\hat{B} \bullet <\vec{S}(0)> = \hat{B} \bullet <\vec{S}(t)>$, so that the component of $<\vec{S}(t)>$ that is parallel to $\vec{B}$ is conserved. Equation 3 also shows that the spins precess in the plane that is perpendicular to $\vec{B}$. This effect is illustrated by the fact that the sum of the final two terms, which equals the component of $<\vec{S}(t)>$ that is perpendicular to $\vec{B}$, is a vector that rotates with a frequency $f_L = \omega_L/2\pi$.

Equation 3 implies that in the presence of $\vec{B}$, the expectation value of the component of the total spin of potentially interacting d's that is perpendicular to $\vec{B}$ is required to vanish periodically as a function of time. As a consequence, by introducing an external field $\vec{B}$, it is possible to induce a preferential orientation such that, in any plane that is perpendicular to $\vec{B}$, the net spin of interacting d's has a greater probability of vanishing than when the spin has a component that is parallel to $\vec{B}$. Since the initial d+d state must have vanishing spin for the excess heat-producing fusion reaction to occur, this implies that by preferentially inducing the spins of potentially interacting d's to rotate, as in Equation 3, there is a greater probability for fusion to occur in any plane that is orthogonal to $\vec{B}$.

Equations 2 and 3 hold rigorously when isolated spins interact only with $\vec{B}$, and not with other magnetic fields. In the presence of other magnetic fields, a more complicated relationship (involving additional Larmor frequencies) is required. In particular, this occurs through coupling between the spin of each d and magnetic fields that are induced by the spin of each electron. However, if an electromagnetic field is also applied in a direction normal to $\vec{B}$, with a frequency $f_L = \omega_L/(2\pi)$, a resonant condition can be established (as in nuclear magnetic resonance) that forces a larger and larger proportion of d-spins to precess, based on the single Larmor frequency ω_L.

Similarly, if a large proportion of spins precess with angular frequency ω_L, electromagnetic radiation possessing a frequency f_L will be emitted in directions normal to an applied magnetic field $\vec{B}$. In the present experiment, the NMR type of configuration, in which an external (RF) electromagnetic signal is applied, was not tested. But, the possibility of electromagnetic emission—with the relevant frequency f_L = 328 kHz, associated with the magnetic field strength (500 G) that was used in the experiments—was monitored. The fact that no appreciable increase in emission was observed at this frequency probably reflects the small concentrations of d's that interact solely with the applied field.

Background About Energy Band Theory and Its Generalization to Finite Solids

Approximate periodic order is known to enhance electronic charge transport in solids, as a result of effects that are associated with energy band states and the wave-like behavior that electrons acquire when they occupy such states. As shown below, this fact may explain why the excess heat is present when $\vec{B}$ is normal to the surface of the electrode and is not present when $\vec{B}$ is parallel to it. In particular, the energy band theory of electrons has been used to explain conductivity in approximately ordered, periodically repeating solids. In the associated theory, conduction occurs through processes that preserve periodic order.

In the generalization of the theory to situations involving finite crystal lattices, the associated process involves a rigid shift (by the same amount) of each of the energies and a comparable shift (by a different amount) of the momentum of each particle that is located in the solid. The associated coherent effect can trigger nuclear reactions through a process in which energy and momentum from the reaction are distributed in a non-local fashion to many different locations at once. Also, this rigid shift can be used to develop a precise formulation of the underlying dynamics associated with enhancements in conduction that occur in periodically ordered metals. This is opposed to the formulation that is used in the conventional theory involving a phenomenological approach in which the effects of boundaries can not be readily incorporated. In the generalization, it follows that the approximate picture associated with the infinite solid is replaced by a more rigorous, quantum mechanical picture in which the presence of currents can be viewed as resulting from a sum of contributions from different energy band states, associated with a different form of wave-like behavior for each state, that can occur when the bulk region is allowed to move rigidly in a coherent fashion, relative to the surface region.

In particular, each energy band state has both a physical momentum $p_{physical}$ and a "crystal momentum" (or "quasi-momentum"[26]) p_i associated with it. In the idealized limit in which the solid remains in its ground state (GS), in the presence of external fields, the rigid motion of the bulk region associated with current flow results from wave-like contributions from each band state. Each of these involves two com-

ponents, in principle. The first one, which does not couple directly to applied $\vec{E}$- and $\vec{B}$-fields, involves a transfer of momentum $\Delta p_{physical} = p_{physical} - p_i = \hbar G_i$ to every unit cell in the bulk. When this occurs, the relative velocity (referred to as the group velocity v_g) between the bulk and surface regions is not altered because G_i, which is referred to as a reciprocal lattice vector,[27] can not alter the GS or any of the lowest lying excited states of the solid. Instead, the resulting difference in momentum, which is transferred directly to the center-of-mass (CM) of the solid as a whole, leads to a combined rigid translation in which both bulk and surface regions move rigidly with the same velocity. The second component, which involves a transfer of the remaining portion of the momentum (p_i) to every unit cell in the bulk region, leads to a rigid shift of the bulk region relative to the surface that results in the flow of current. The different forms of momentum transfer, which are restricted in this way in order to minimize energy, occur because in the bulk region each unit cell is required to be neutral; this is not true in the surface region and, as a result, charge does not have to be conserved (which is the case when current flows between different portions of the surface region that are separated from each other by the bulk region).

The associated coherent effect, which involves a transfer of momentum from the external environment into the interior, is based on the governing principles that are associated with the kinds of rigid lattice recoil effects that cause the Mossbauer effect. As we will see, when currents are not altered as a result of the momentum transfer to the CM of the entire solid (which occurs from the contribution associated with $\Delta p_{physical} = p_{physical} - p_i = \hbar G_i$), the associated rigid motion (which can still take place when applied external fields are introduced) has important implications associated with the most coherent forms of interaction, and these can induce nuclear fusion.

In either the original theory or its generalization,[11,16] the current density $\vec{j}(r)$ at any location, associated with an electron (in an electron energy band state) or ion (in an IBS) possessing charge $q = \pm e$ inside the solid is given by a sum over individual energy band current (IEBC) contributions. Each of these is defined by a current from a "wave-like" particle (also referred to as a "quasi-particle") associated with each value of the "quasi-momentum" p_i and the particular value of the energy ε_α associated with a particular energy band value $\varepsilon_a \equiv \varepsilon_a(p_i)$. These IEBC contributions are constructed from the product of the group velocity $v_g(\varepsilon_\alpha(p_i))$, which is defined by $v_g(\varepsilon_\alpha(p_i)) = \nabla_{p_i}\varepsilon_\alpha$, with the change in the probability density $\delta G_B(r, p_i, \varepsilon(p_i))$ that the particular energy band value will become occupied when (constant) external electric and/or magnetic fields are applied:

$$j(r) = \frac{q}{N_{cell}V_{cell}} \sum_{i,\alpha} \delta G_B(r, p_i, \varepsilon_\alpha(p_i)) \nabla_{p_i}\varepsilon_\alpha(p_i) \ , \qquad (4)$$

where N_{cell} is the number of unit cells in the lattice and V_{cell} is the volume of each unit cell. Also, in Equation 4, $p_i = \hbar k_i$, where each wave-vector k_i is restricted to the First Brillouin Zone (FBZ).[11,16,28] Each term in the sum (Equation 4) can be viewed as arising from an IEBC contribution because it can be re-defined using the expression $v_g\rho_\alpha(r) \equiv v_g(\varepsilon_\alpha(p_i)) \times \delta G_B(r, p_i, \varepsilon_\alpha(p_i))$, where $\rho_\alpha(r) \equiv \delta G_B(r, p_i, \varepsilon_\alpha(p_i))$ is the density associated with a particular energy band state that is created in response to the applied electromagnetic field, and $v_g(\varepsilon_\alpha(p_i)) = \nabla_{p_i}\varepsilon_\alpha(p_i)$ is the associated velocity of the contribution.

In the semi-classical treatment of transport phenomena associated with conventional energy band theory in infinitely-repeating solids, both v_g and $\rho_\alpha(r)$ have been defined heuristically, based on a "picture" in which each particle that occupies an energy band has an effective density $\rho_\alpha(r) = f(\varepsilon_\alpha(p_i),T)\times|\Psi_{\varepsilon_\alpha}(r)|^2$. That density is defined by a thermal factor $f(\varepsilon_\alpha,T)$ associated with a quantum mechanical "gas" of non-interacting (boson or fermion) quasi-particles, which is constructed from single particle wave functions $\Psi_{\varepsilon_\alpha}(r)$. These solve a "quantum mechanical" (Schrödinger) equation, associated with a periodic potential.

Although the possible functional forms for $\Psi_{\varepsilon_\alpha}(r)$ and v_g can be viewed as being constructed quantum mechanically, the actual transport behavior associated with these quantities does not "appear" to involve quantum mechanics directly. In particular, transport phenomena are associated with the flow of charge, as a function of time. In order to introduce the time dependence associated with this, a "semi-classical" approach is used to model the behavior of $\nabla_{p_i}\varepsilon_\alpha(p_i),\varepsilon_\alpha(p_i)$ (and implicitly $\Psi_{\varepsilon_\alpha}(r)$), as a function of time in a manner that is not quantum mechanical. This is accomplished by "assuming" that the momentum variable p_i evolves dynamically, using an "effective Lorentz force" equation of motion.

In particular, in this semi-classical approach, the external electromagnetic fields, $\vec{E}$ and $\vec{B}$, introduce effective forces that alter the group velocity v_g and the quasi-momentum p_i of each of the quasi-particles in each energy band, based on the following "rule": when the initial value of the quasi-momentum is p_i and the initial value of the energy is $\varepsilon_\alpha(p_i)$, the value of ε_α changes with time through the relationship, $\varepsilon_\alpha \equiv \varepsilon_\alpha(t) \equiv \varepsilon_\alpha(p_i(t))$, where $p_i(t)$ obeys

$$\frac{dp_i(t)}{dt} = q\vec{E} + \frac{q}{c}\ v_g(\varepsilon_\alpha(p_i)) \times \vec{B} \ , \qquad (5)$$

In the case of electrons, as the temperature T approaches zero (because the thermal factor $f(\varepsilon_\alpha(p_i),T)$ approaches a step function $\theta(\varepsilon_F - \varepsilon_\alpha(p_i))$ that vanishes when $\varepsilon_\alpha(p_i)$ is greater than or equal to the Fermi energy ε_F), both v_g and $\rho_\alpha(r)$ are determined, using Equation 4, from the unoccupied wave functions and energy bands that result from this procedure.

Because this conventional picture is associated with current flow, the quasi-momentum is always used to define how v_g changes. The physical momentum is never precisely related to the flow of currents, and the implicit form of coherent, rigid motion that is involved in the effect is not immediately obvious. However, as mentioned above, in the alternative formulation,[11,16] a more precise interpretation exists, in which each IEBC contribution occurs from this kind of effect. In particular, in situations involving the GS, and the lowest lying excitations, the analysis[16] shows that each IEBC contribution results from a process in which the bulk region "moves" rigidly in response to an applied electric field. The same argument also shows that in this limit the bulk region "moves" rigidly in response to an applied magnetic field, and the associated rigid forms of motion are actually responsible for Equation 5.

These facts are implied by the argument that leads to Equation 4 when the complete quantum mechanical problem is applied, associated with situations in which particles within the bulk region have the lowest rates of interaction with the environment. In this limit, perturbations from the

outside environment can occur that do not alter the distribution of charge or any of the separations between charges in the bulk. The flux of particles that enter the solid causes all of the momenta of the particles in the bulk to shift by the same constant amount. Such a change does not alter how particles within the bulk region collide with each other or with the environment, since it is never possible to determine if this region is in motion or at rest, relative to its environment. For this reason, the absolute energy and total momentum of the solid are never known, and the lowest values of the energy and momentum (the zeroes of energy and momentum) of the solid are never known.

By requiring that the many-body wave functions associated with the lowest GS energy and the lowest energies of the solid not be altered by changes in the zero of momentum, it is possible to establish the time evolution of the zero of momentum, associated with the lowest energies of the solid, in the presence of constant applied $\vec{E}$- and $\vec{B}$-fields.

Within this context, variations in velocity can be rigorously interpreted as arising from variations in the motion of the quasi-particles[11,16] associated with rigid motions of the bulk solid relative to the surface. The separation between each pair of particles remains fixed. It is possible to show[11,16] that the group velocity of each IEBC contribution actually equals the GS velocity of the rigid motion of the entire bulk region relative to the boundary of the solid. The velocity results when the same amount of physical momentum $p_{physical} = p_i = \hbar k_i$ is transferred to each unit cell in the bulk.

Two key points associated with Equation 5 that result from this more precise interpretation are: 1) It is possible for the rigid motion to induce coherent, resonant forms of momentum transfer, into and away from the solid, that are completely elastic; 2) It is possible to quantify the limiting effects associated with collisions that inhibit the effective rigid motion. In particular, as t becomes sufficiently large, coherent resonant forms of momentum transfer can take place when the time integration of the right side of Equation 5 approaches $\Delta p_{physical} = \hbar G_i$. The limiting effects associated with collisions that potentially inhibit these forms of coherence are implicit in the thermal averaging (associated with Equation 4) used in the conventional picture associated with quasi-particles in metals.

In general, the coherent effect associated with rigid motion of the bulk is suppressed over longer periods of time, as a result of collisions that result from the accumulation of charge in the boundary regions. Their effects are hidden as a result of the thermal averaging. However, at reduced T, in one notable situation, this does not have to be the case: When the solid is an insulator (which occurs when the highest occupied band is filled or $\nabla_{p_i}\varepsilon_\alpha(p_i) = 0$). In this kind of situation, collisions can be suppressed, in principle, to such an extent that in the idealized limit in which the solid remains near its GS, it can become possible for

$$\int_0^t dt' \, \frac{dp_i(t')}{dt'} \rightarrow \nabla p_{physical} = \hbar G_i = \vec{E}\, t \,, \qquad (6)$$

in a coherent fashion (as discussed below).

Bloch[29] suggested the possibility of a different kind of effect taking place in normal metals, in situations involving Equation 6. In particular, he noticed that when $\vec{B} = 0$, Equation 5 suggests that if Equation 6 is satisfied, oscillations (referred to as Bloch oscillations) in the quasi-momentum p_i of the quasi-particles would take place. The frequency (referred to as the Bloch oscillation frequency) $f_{Bloch} = 2\pi/\tau_{Bloch}$ of these oscillations is defined by the smallest value of $t = \tau_{Bloch}$ associated with Equation 6. (This occurs when G_i is the smallest reciprocal lattice vector that is parallel to $\vec{E}$ in Equation 6.) Zener[30] suggested that in an insulator or semiconductor, through Equation 6, physical momentum should be imparted to the actual charge within the solid to such an extent that tunneling to different energy bands should become possible.

Mechanism for Triggering Nuclear Fusion in Finite Solids

In the more rigorous analysis,[11,16] Equation 5 describes the change in the zero of momentum in the limit in which Equation 6 applies. Collisions are suppressed, and every unit cell in the bulk region acquires this amount of momentum. Using this fact, it is possible to identify a triggering time for a potential coherent form of momentum transfer. It is associated with the possibility that the solid as a whole moves with a velocity that matches the velocity that would be induced as a result of a nuclear fusion reaction. Such a reaction could result from the overlap between two d's that occupy IBS's. In particular, in a situation in which even a small amount of momentum Δp_{small} is transferred to each unit cell, a total amount of momentum $p_{total} = N_{cell}\Delta p_{small}$ is transferred to the entire lattice. Actually, in the presence of collisions, it is never possible to determine if p_{total} is transferred to a single point, to many points or to all of the points in the solid.

In the limit of a small number of collisions, two equivalent pictures are applicable: 1) One can focus on all of the lattice sites at once and conclude that as a result of Equation 5, with increasing t, every unit cell simultaneously acquires the same change in quasi-momentum, over some finite time, defined by the smallest interval of time between collisions; or 2) One can focus on a single unit cell, allowing for the possibility that at any time a collision can take place, on any time scale, and that any amount of quasi-momentum can be transferred to the unit cell. In both situations, eventually, a total amount of momentum $N_{cell}\,\hbar G_i$ will be transferred to the lattice. How this occurs can be viewed as resulting from a situation in which an amount of momentum $p_{total} = \hbar G_i$ is transferred to a single unit cell N_{cell} different times or to m different cells, N_{cell}/m times. In the most general situation, the momentum is transferred first to m_j different cells, a particular number (N_j/m_j) times, then to a different number (m_j') of cells, N_j/m_j' times, followed by a different number of cells, a different number of times, sequentially, in such a way that $N_{cell} = \sum_j N_j$.

Quantum mechanics in the absence of collisions requires that it is never possible to distinguish between the situation when the transfer occurs only in one unit cell, or a second unit cell, or in any other cell, any number of times, all of these pictures are equivalent. In this context, in the original picture suggested by Bloch, whenever a Bloch oscillation occurs, the resulting transfer of momentum can be viewed as occurring in a single unit cell and involving a single amount of momentum $p_{total} = \hbar G_i$, where G_i is the smallest reciprocal lattice vector in a particular direction, in one unit cell. That can be followed (as a result of a second oscillation) by a second transfer of the same amount of momentum, in the same place, followed by a third transfer, and so forth. In this way, it can be seen that through Bloch's picture, sequentially, the

momentum that is transferred can grow with time, until finally a total amount $p_{total} = N_{cell}\hbar G_i$ is transferred to the lattice. But equivalently, it also follows that all of the associated transfers of momentum can take place in every unit cell, incrementally in small amounts, in such a way that the total transfer occurs in a single Bloch oscillation, but in every unit cell.

An important point is that the associated picture establishes a guideline for estimating a bound for the largest amount of momentum that can be transferred to the lattice, without creating a collision. It is worthwhile recognizing that although Bloch suggested that an oscillation in the quasi-momentum of each quasi-particle would take place every time p_i approaches the boundary of the FBZ,[28] in fact what actually *is supposed to happen* is that when p_{total} reaches this boundary, *it is supposed to change* discontinuously (by an amount equal to a reciprocal lattice vector) in such a way that it acquires a different value, associated with a different location on the FBZ boundary. As a consequence, in the absence of an applied magnetic field, the change in physical momentum

$$\Delta p_{physical} = e\vec{E}\,\Delta t \qquad (7)$$

in each unit cell that results when the constant $\vec{E}$-field is applied over a time Δt monotonically increases, and p_i does not oscillate when it reaches a zone boundary. Rather, it shifts its value. In particular, for example, if $\vec{E}$ is parallel to p_i and G_i, in the limit that p_i approaches $p_i = \hbar G_i/2 - \varepsilon\hbar G_i$, with increasing time it suddenly shifts to a new value $p_i = \hbar G_i/2 + \varepsilon\hbar G_i$. Then, the CM of the lattice, as a whole, acquires the missing momentum $\Delta p_{cm} = \hbar G_i$.

In order to have the least coupling to the environment, every time p_i changes in this way, the lattice as a whole can either move rigidly, or the change in momentum can lead to one or more elastic processes in which the associated change becomes distributed to different locations. Because of this, it is possible for collisions to take place, but since in this limit they are required to conserve energy, these collisions involve reversible processes. When this occurs in the limit in which $p_{total} \to N_{cell}\hbar G_i$, the entire solid (including the bulk and surface regions) must move rigidly. Although the associated process can, in principle, also be reversible, coupling to the electromagnetic field (resulting in the creation of phonons and lattice vibrations) is also required as a result of accumulations of charge in the surface region (as well as at locations of lattice imperfections). As a consequence, although at temperature T=0, as $p_{total} \to N_{cell}\hbar G_i$, it is still possible for any additional momentum that is transferred to charged particles in the lattice (according to Equation 5) to result entirely in elastic processes. At any finite value of T, the associated effect must induce phonons.

In situations involving electrons, because of the Pauli exclusion principle, the collision-less limit can only involve changes in the current that result from changes in the values of $p_{physical}$ and p_i that are associated with the single, highest occupied energy band. Because a large number of different energy states are involved in this band, a large volume of phase space (associated with different values of the wave-vector) is available. Hence, the possible effects associated with the most coherent forms of coupling (which occur through Bloch oscillations) do not have a noticeable effect in metals. This is not entirely true in insulators and semi-conductors. In particular, although in conventional insulators and semi-conductors Bloch oscillations (and Zener tunneling) have not been observed, these phenomena have been created in artificial environments.[31,32]

In the situation in which d's occupy the lowest energy IBS's, when there are no collisions (which occurs when T=0) they form a Bose Einstein Condensate (BEC). Then, they all occupy a single state. For this reason, the available phase space for supporting collisions is greatly reduced. In the absence of collisions and applied magnetic fields, the single GS wave function that the d's occupy is required to have vanishing quasi-momentum, initially. As a function of time, the value of its quasi-momentum constantly changes, through Equation 7, according to the equality $\Delta p_{physical} = \Delta p_i$ in every unit cell (until the wave-vector of p_i approaches the boundary of the FBZ).

Although this collision-less limit is not physical, it defines a lower limit for the potential reaction rate. In particular, collisions must occur when momentum is lost to the external environment. For a sufficiently large crystal, this takes place when the boundary and bulk both are required to move rigidly after a critical time, t_{crit}. That time occurs when each value of p_i has a wave-vector that is located on the Brillouin Zone boundary. When this happens, the CM acquires a momentum $p_{cm} = N_{cell}G_i\hbar$. Elsewhere, Chubb has suggested[33,34] that if N_{cell} becomes sufficiently large, the associated transfer of momentum can potentially trigger nuclear reactions. Implicit in this idea is the requirement that the GS has minimal coupling to the environment. This occurs in the interesting limit that becomes possible when the momentum from a potential d+d→^{4}He is transferred electromagnetically directly to the CM of the lattice:

$$p_{cm}c = N_{cell}G_i\hbar c = 23.8 \text{ MeV} . \qquad (8)$$

Effectively, when N_{cell} approaches infinity, the associated process can be viewed as occurring when the momentum of the γ ray that would be created in the conventional d+d→^{4}He + γ reaction is distributed between N_{cell} photons, each with an energy 23.8 MeV/N_{cell} (and momentum 23.8 MeV/($N_{cell}c$); c=speed of light). The energy and momentum become vanishingly small as N_{cell} becomes sufficiently large.

In regions where d's can potentially have overlap, it must be possible for both a net (but small) accumulation of charge and for a potential change in the zero of momentum to occur (through the change in mass associated with a potential d+d→^{4}He reaction). As a result of this possibility, in the limit in which the GS and lowest lying excited states have the smallest overlap with the environment and with each other, in the small (nuclear dimension) region of each unit cell where the overlap can occur between d's, the value of the possible relative momentum between d's is allowed to shift abruptly in order to minimize (and suppress) collisions. In the idealized collision-less limit, in which the solid is allowed to move rigidly in response to external fields (as in Equations 5 and 7), and each d is approximated as a point particle, these abrupt changes are replaced by discontinuous changes. When this is allowed to take place, it is possible to have appreciable overlap between d's by requiring that collisions be inhibited from taking place through a process that minimizes energy.[24]

As a consequence, it is possible for sufficient overlap to

occur for a nuclear reaction to take place. Equation 8 can be satisfied and used to identify a limiting value for the lowest (finite) rate of any nuclear fusion process involving the d+d→^{4}He reaction, associated with a particular crystal size. The model can be used to estimate minimal values of N_{cell} and t_{crit} for the size and critical time that are required for this to occur. In situations involving electrons, the electric and magnetic fields that are associated with Equations 5 and 7 are the physical, external fields that are applied to the solid. Because in the situation involving d's the occupation of IBS's in larger crystals of PdD are induced by fluctuations in loading, it is more appropriate to treat the associated fields as being induced as a result of the behavior of the electrons that result from these changes.

Chubb[33,34] used an estimate of the induced $\vec{E}$-field (~1x10^{-8} eV/$\mathring{A}$) that is consistent with comparable fields in macroscopic PdD crystals to determine an approximate value of N_{cell} and t_{crit} in nanometer scale crystals. In these calculations, as opposed to transferring momentum electromagnetically directly to the solid (through Equation 8), a slightly different model is used. In that model the transfer occurs through ^{4}He nuclei that occupy IBS's. But this last model implicitly involves greater coupling to the external environment since the IBS's associated with the ^{4}He nuclei that would be involved in this form of coupling are required to have higher energy than the GS. When the more rigorous model (involving Equation 8) is used, the resulting minimal value (N_{min}) for the number of unit cells in the bulk region is N_{cell}=N_{min}=5,560. By applying Equation 7 N_{min} times, it is possible to determine t_{crit} using the relationship

$$\Delta p_{cm} = \vec{E}\, t_{crit} = \vec{E}\, N_{min}\tau_{Bloch} = N_{min}\Delta p_{physical} = N_{min}\hbar G_i\ , \quad (9)$$

where both equalities result from the requirement that $\Delta p_{physical} = \hbar G_i$ simultaneously in each unit cell, in the limit that $p_i/\hbar = \vec{k}_i$ also simultaneously becomes equal to a wavevector that is located on the boundary of the FBZ. In particular, in this limit each unit cell contributes a change in the amount of momentum $\Delta p_{physical} = \vec{E}\,\Delta t = \vec{E}\,\Delta\tau_{Bloch} = \hbar G_i$, where G_i is one of the three reciprocal primitive vectors[35] of the FCC lattice. The second equality holds as a result of the definition of τ_{Bloch}. Equation 9 leads to

$$t_{crit} = N_{min}\,|G_i|/(e|\vec{E}|) = N_{min}2\pi\,\sqrt{3}\,/(e|\vec{E}|a), \quad (10)$$

where a = 4.09$\mathring{A}$ is the (beta phase) PdD lattice constant. Substituting the value $\vec{E}$ = 1 V x 10^{-8}/$\mathring{A}$ that was used previously,[33,34] we find that t_{crit} = 0.98 ms. Equation 9 also implies that the critical time required for nuclear reaction occurs when

$$t_{crit} = N_{min}\Delta t = N_{min}\tau_{Bloch}\ . \quad (11)$$

A comparable effect can trigger collisions (and a nuclear reaction) in larger crystals, in which the number of unit cells $N'_{cell} \geq N_{min}$. In this situation, the associated critical time t'_{crit} obeys a modified version of Equation 11, in which N_{min} is replaced by N'_{cell}. As a consequence of this last relationship, it follows that

$$t'_{crit} = t_{crit} \times N'_{cell} / N_{min} = N'_{cell}\tau_{Bloch}\ . \quad (12)$$

Equations 11 and 12 have important implications because collisions are suppressed when $t < t_{crit}$ ($t < t'_{crit}$) in crystals that have N_{min} (N'_{cell}) unit cells. In particular, it follows from these two equations that in larger crystals in the most coherent limit, the time for any nuclear reaction to occur can increase dramatically. Specifically, as the characteristic dimension of a crystal increases by a factor of 10, Equation 12 implies that the time delay before a nuclear reaction is triggered increases by a factor of 1,000. The smallest crystal that can sustain a fusion reaction through the most coherent process has a characteristic dimension a ~0.45 nm, requires a triggering time $t_{trig} = t_{crit}$ ~1 ms. In a crystal that has a value of a ~0.45 μm that is 1,000 times greater, t_{trig} is on the order of a billion times larger (~18 days). The value of t_{trig} that corresponds to six weeks (the time that was required in a number of the initial excess heat experiments) is associated with a crystal that has a characteristic dimension a ~7 μm.

In fact, many forms of collisions can take place, leading to rapid coupling between the ^{4}He product and the external environment. These estimates for t_{min} and N_{min} are consistent with the requirement that periodic order be preserved in the bulk region, over a time-scale that is longer than the time that is required for the nuclear energy and momentum from the reaction to be transferred to the lattice. This is necessary in order for IBS's to be involved in the process. The estimates and underlying picture are also consistent with the requirement that energy be minimized within the bulk region. An important point is that because the collision-less limit that is the basis for these estimates results from an electromagnetic interaction, the presence of any collision that involves conventional excitations of the solid (including phonons, plasmons, electronic excitations, etc.) implicitly leads to a form of electromagnetic coupling between the associated nuclear reaction and the environment that can induce enhancements in fusion reaction rate provided they do not significantly inhibit either d-d overlap or the expulsion of ^{4}He from the bulk. For example, in a separate calculation, recently Chubb and Chubb have shown[24] that appreciable overlap can take place between d's that occupy IBS's when N_{cell} is as small as ~650, corresponding to a crystal possessing a characteristic dimension a ~2 μm. In principle, in a crystal of this size in the presence of collisions, electromagnetic coupling through "photons" associated with the final state in the d+d→^{4}He reaction can occur directly via a process that involves a continuum of possible wavelengths, ranging from the situation (associated with localized forms of interaction) involving gamma rays, to more distributed, delocalized reactions that can result in hard X-rays, soft X-rays, infra-red, optical, microwave, RF and lower frequency emission of electromagnetic radiation. However, these emissions probably are significantly stifled in larger crystals and are not expected in most situations involving IBS's, except in smaller nm scale crystals.

The emissions potentially could be initiated from a coherent effect associated with either the kind of order-preserving limit that leads to the limiting value $N_{cell} = N_{min}$, or through a comparable order-preserving situation (for example, when $N_{cell} = 650 < N_{min}$) where N_{cell} is large enough for appreciable overlap to take place but not large enough to trigger a nuclear reaction, through processes that are related to the collision-less limit. In particular, in this last situation, because the process in which momentum is transferred to the lattice is coherent, the emission could be coherent. For example, it might involve a large number (n) of photons

(potentially as many as $n = N_{cell}$ photons), in which each photon possesses a frequency

$$f = \frac{23.8 \text{ MeV}}{hn} \quad (h \text{ is Planck's constant}).$$

When $n = N_{cell} = 650$, each of the n photons would be emitted as a hard (366 KeV) X-ray, while for the limiting case involving the smallest crystals where the most coherent form of triggering occurs, $n = N_{min} = 5560$, and each of the resulting n photons would be a softer (42.8 KeV) X-ray.

Although in principle these X-rays would be emitted coherently, because the concentrations of potentially interacting d's is small, the net flux of photons that would be emitted is also small. The fact that they could be coherent would probably be difficult to observe. It is possible that the hard X-rays that have been observed in the SPAWAR co-deposition experiments could be related to these kinds of emissions.

Because the dominant forms of interaction should be associated with the GS and the lowest energy excitations, the processes that have the greatest effect should be associated with the approximate limit in which collisions are "stifled." The most important of these involve overlap and interaction between the GS and states that are nearest in energy with the GS which have the greatest number of states with the same or nearly the same energy (the states that are most degenerate or nearly-degenerate).

Because of the need to preserve periodic order in bulk regions, a pivotal form of degeneracy occurs through processes associated with the kind of rigid motion that can be initiated when the quasimomenta $p_i = \hbar\vec{k}_i$ has a wave-vector $\vec{k}_i$ that is located on the boundary of the FBZ. This is a special case of a more general phenomenon that occurs in bulk regions: As a function of p_i, the energy ($E(p_i)$) of any IBS [where $E(p_i)$ is an IBS energy $\varepsilon(p_i)$], electron [where $E(p_i)$ is the energy of an energy band state], or phonon [where $E(p_i) = \hbar\Omega(p_i)$ is the energy of a phonon possessing angular frequency $\Omega(p_i)$] is required to possess a degeneracy:

$$E(p_i) = E(p_i + \hbar G_n) \,, \tag{13}$$

where G_n is any arbitrary reciprocal lattice vector.

In the general formulation[16] of band theory, the associated degeneracy applies both to energy band states and phonons. That is the case because it is a result of the requirement that the GS and the lowest-lying excitations preserve periodic order and involve changes in quasi-momentum $p_i = \hbar\vec{k}_i$ associated with the fact that the zero of momentum is allowed to change (in order to preserve periodic order and minimize the energy) until the associated wave-vector approaches the boundary of the FBZ. There it shifts by one of the reciprocal primitive vectors G_1, and the solid moves rigidly by absorbing a compensating amount of momentum, $\hbar G_1$, in the opposite direction. Thus, the shift in quasi-momentum and rigid motion of the lattice that results from this is actually a general, coherent effect that applies not only to the potential Bloch oscillations associated with d's in IBS's but to phonons and (in principle) to electrons that occupy energy band states (where the effect is also referred to as a Bloch oscillation).

An important point, however, is that although in principle the degeneracy associated with Equation 13 suggests that many states can have the same energy, the ones that are involved in a particular process have to conserve total energy and momentum. The coherent process associated with the collision-less limit, in which appreciable momentum can become distributed (as a consequence of the changes in the zero of momentum) through Equations 5 and 7, provides a form of coupling that can make this possible. As a consequence of this fact, in the presence of collisions (as a result of Equation 13) significant coupling between IBS's involving d's and ^{4}He with phonons can also take place either coherently or incoherently, provided the physical momentum is conserved in bulk regions.

The potential coupling through a more general form of Equation 13 can also occur in surface regions, in a 2-dimensional (2D) limit, involving approximate 2D periodic symmetry in planes that are parallel to the surface. In this situation, as opposed to the situation involving a 3-dimensional (3D) reciprocal lattice vector, G_n becomes 2D (defined by the 2D lattice). In smaller crystals, forms of coupling between IBS's involving d's and ^{4}He with phonons, through the kinds of processes associated with Equation 13 (either in 2D or 3D situations), are the dominant modes of interaction that suppress electromagnetic radiation emission.

The Role of $\vec{B}$ Field Orientation in the Triggering Process

When an external $\vec{B}$-field is introduced, the possible accumulation of momentum that can trigger the nuclear reaction appears to be strongly dependent on the orientation of the field. In particular, when an external $\vec{B}$-field is introduced into Equation 5, the associated form of triggering acquires a directional dependence that appears to be relevant to the fact that excess heat does occur when $\vec{B}$ is perpendicular to the electrode, but it is not present when $\vec{B}$ is parallel to it. As we will show using the solutions of the resulting expression, the coherent effect that triggers the reaction can occur in an unimpeded fashion when $\vec{B}$ is parallel or anti-parallel to the $\vec{E}$-field which initiates the effect, and this occurs when $\vec{B}$ is normal to the surface. But when the $\vec{B}$- and $\vec{E}$-fields are perpendicular to each other, the triggering effect becomes suppressed because in directions that are perpendicular to $\vec{B}$, the presence of $\vec{B}$ constrains the effective force that interacts with each potentially interacting d to move in a circular pattern; in directions parallel to $\vec{B}$, there is no force and, as a consequence, when $\vec{B}$ is parallel to the electrode, triggering does not take place.

The accumulation of momentum can occur because, as a consequence of Equation 7 for the situation in which $\vec{B} = 0$, the presence of $\vec{E}$ causes $\nabla p_{physical}$ to increase monotonically. For this reason, in principle, in the absence of collisions, as t increases without bound, the magnitude of $\nabla p_{physical}$ can also increase without bound. Using Equation 5, it is possible to show that a similar effect can occur when in addition to $\vec{E}$, an external $\vec{B}$-field is introduced, but only when $\vec{B}$ is not perpendicular to $\vec{E}$. In particular, Equation 5 implies that

$$\frac{d\hat{B} \bullet p_i(t)}{dt} = q\hat{B} \bullet \vec{E} \tag{14}$$

Using the notation, $\vec{B} = \vec{B}_\perp$, when $\vec{B}$ is perpendicular to $\vec{E}$, and $\vec{B} = \vec{B}_\parallel$ when $\vec{B}$ is parallel to $\vec{E}$, it follows from Equation 14 that since

$$\frac{d\vec{B}_\perp \bullet p_i(t)}{dt} = 0 \,,$$

the component of $p_i(t) = \hat{B}_\perp \hat{B}_\perp \bullet p_i(t)$ that is parallel (or anti-parallel) to $\vec{B}_\perp$ is conserved:

$$\hat{B}_\perp \bullet p_i(t) = \hat{B}_\perp \bullet p_i(0) \ . \tag{15}$$

(Here, as in Equation 2, $\hat{B}_\perp = \vec{B}_\perp / |\vec{B}_\perp|$.) But when $\vec{B} = \vec{B}_\parallel$, Equation 14 implies that

$$\frac{d\vec{B}_\parallel \bullet p_i(t)}{dt} = \pm |\vec{B}_\parallel||\vec{E}| \ ,$$

where the plus or minus sign, respectively, is used when $p_i(t)$ is parallel or anti-parallel to $\hat{B}_\parallel$. In this case,

$$\hat{B}_\parallel \bullet p_i(t) = \hat{B}_\parallel \bullet p_i(0) \pm |\vec{E}| t \ . \tag{16}$$

Equations 15 and 16 show that when $\vec{B}$ is parallel to $\vec{E}$, the magnitude of the component of $p_i(t)$ that is parallel to $\vec{B}$ monotonically increases with time, while in the situation in which $\vec{B}$ is perpendicular to $\vec{E}$, the magnitude of the component of $p_i(t)$ that is parallel to $\vec{B}$ remains constant. This fact suggests that whether or not the triggering effect occurs depends on the orientation between $\vec{B}$ and $\vec{E}$. In particular, when $v_g(\varepsilon_a(p_i)) = \nabla_{pi}\varepsilon_a$ is parallel to $p_i(t)$, changes that occur in $p_i(t)$ from the presence of $\vec{B}$ are always perpendicular to $p_i(t)$ and $\vec{B}$. In a large number of cases, the magnitude of the component of $p_i(t)$ that is perpendicular to $\vec{B}$ never deviates significantly from its initial value. For this reason, the fact that $\hat{B}_\parallel \bullet p_i(t)$ grows monotonically when $\vec{B}$ is parallel to $\vec{E}$, while it remains constant when $\vec{B}$ is perpendicular to $\vec{E}$, suggests that when $\vec{B}$ is parallel to $\vec{E}$ in the "collision-less" limit, $p_i(t) = \hbar k_i(t)$ can increase simultaneously in each of the N_{cell} unit cells to the point that each value of $k_i(t)$ approaches the boundary of the FBZ. This leads to a situation in which a fusion reaction is triggered, as in the situation that can occur when $\vec{B} = 0$; when $\vec{B}$ is perpendicular $\vec{E}$, this cannot take place.

This observation can be quantified by considering a useful example which applies for a large number of situations. The example also shows rigorously that in the most coherent limit (in which all of the d's initially occupy the single, lowest, IBS, with $k_i(0)=0$), when $\vec{B}$ is perpendicular to $\vec{E}$, the magnitude of $p_i(t)$ never becomes appreciable. But, it grows in a manner that is proportional to t when $\vec{B}$ is perpendicular to $\vec{E}$. The example involves assuming that $\varepsilon(p_i)$ can be represented using the relationship

$$\varepsilon(p_i) = \varepsilon_0 + \frac{p_i^2}{2m_{eff}} \equiv \varepsilon_0 + \frac{\hbar^2 k_i^2}{2m_{eff}} \ , \tag{17}$$

where ε_0 is a constant (= $\varepsilon(0)$), and

$$m_{eff}^{-1} \equiv \left[\frac{\partial^2 \varepsilon}{\partial p_x^2} + \frac{\partial^2 \varepsilon}{\partial p_y^2} + \frac{\partial^2 \varepsilon}{\partial p_z^2} \right]\Big|_{\vec{p}=0} \tag{18}$$

is referred to as the inverse of the effective mass. Equations 17 and 18, which are used frequently in models of semi-conductors, provide an exact representation of an arbitrary (lowest energy) energy band for a crystal that possesses cubic symmetry (which applies to the situation associated with Pd and PdD), in the limit that $p_i = \hbar k_i \to 0$.

When Equation 17 is used to evaluate

$$\nabla_{\vec{p}} \varepsilon = \frac{p_i}{m_{eff}} = \frac{\hbar k_i}{m_{eff}}$$

and substituted into Equation 5, the resulting expression is:

$$\frac{dp_i(t)}{dt} = q\vec{E} + \omega_c p_i(t) \times \hat{B} \ , \tag{19}$$

where

$$\omega_c = \frac{q|\vec{B}|}{m_{eff}}$$

is an effective "cyclotron" frequency. In analogy with the free space cyclotron frequency, it defines the angular frequency of the circular orbits that are the solutions of Equation 19 when $\vec{E} = 0$. Although the solutions of Equation 19 are not circular orbits when $\vec{E} \neq 0$, the physical effect that is responsible for the circular orbits has a residual effect on how p_i changes with time. In particular, the solutions are circular orbits when $\vec{E} = 0$ because for this case, the changes in the trajectory of p_i that are induced by $\vec{B}$ are always perpendicular to p_i.

When $\vec{E} \neq 0$, $\vec{B}$ also induces changes that are always perpendicular to p_i. For this reason, the component ($p_\perp^{perp}$) of p_i that is perpendicular to $\vec{B}$ is always constrained so that it cannot increase without bound. In particular, when $\vec{B} = \vec{B}_\parallel$, the effective force that acts on $p_\perp^{perp}$ (rate of change of $p_\perp^{perp}$ with respect to time) rotates in a circle with angular frequency ω_c,

$$\frac{dp_\perp^{perp}(t)}{dt} = \frac{dp_\perp^{perp}(0)}{dt} \cos(\omega_c t) + \frac{dp_\perp^{perp}(0)}{dt} \times \hat{B}_\perp \sin(\omega_c t). \tag{20}$$

When $\vec{B} = \vec{B}_\parallel$, the comparable component ($p_\parallel^{perp}$)rotates in a circle with the same angular frequency:

$$p_\parallel^{perp}(t) = p_\parallel^{perp}(0)\cos(\omega_c t) + p_\parallel^{perp}(0) \times \hat{B}_\parallel \sin(\omega_c t) \ . \tag{21}$$

From Equations 16 and 21, it is possible to show that when $\vec{B} = \vec{B}_\parallel$, as a function of time, $p_i(t) = p_\parallel(t)$, is given by

$$p_\parallel(t) = \hat{B}_\parallel(\hat{B}_\parallel \bullet p_i(0) \pm |\vec{E}|t) + p_\parallel^{perp}(0)\cos(\omega_c t) + p_\parallel^{perp}(0) \times \hat{B}_\parallel \sin(\omega_c t). \tag{22}$$

This implies that (as in Equation 7) the magnitude of $p_\parallel(t)$ increases without bound as t increases:

$$|p_\parallel(t)| = \sqrt{(\hat{B}_\parallel \bullet p_\parallel(0) \pm q|\vec{E}|t)^2 + |p_\parallel^{perp}(0)|^2} = |p_\parallel(0) + q\vec{E}t| \ . \tag{23}$$

Similarly, using Equations 15, 19 and 20, it follows that

$$p_\perp(t) = p_\perp^{perp}(0) + (q\vec{E} + \omega_c p_\perp^{perp}(0) \times \hat{B}_\perp) \frac{sin(\omega_c t)}{\omega_c} + (q\vec{E} + \omega_c p_\perp^{perp}(0) \times \hat{B}_\perp) \times \hat{B}_\perp \left(\frac{1-\cos(\omega_c t)}{\omega_c}\right) \tag{24}$$

which implies that $|p_\perp(t)|$ can be written in the following form:

$$|p_\perp(t)| = (|p_\perp^{perp}(0)|^2 + 2\{q^2|\vec{E}|^2 - q\omega_c p_\perp^{perp}(0) \bullet [\vec{E} \times \hat{B}_\perp]\}(1 - \cos(\omega_c t))/\omega_c^2 + 2p_\perp^{perp}(0) \bullet \vec{E} \sin(\omega_c t)/\omega_c)^{1/2} \ . \tag{25}$$

Because when the interacting d's all occupy the lowest IBS, initially the quasi-momenta (and wave-vectors) all vanish in this limit, it follows from Equations 23-25 that

$$|p_\perp(t)| = 2q \left| \frac{\vec{E} sin(\omega_c t/2)}{\omega_c} \right| \ , \tag{26}$$

and

$$|p_{\|}(t)| = q|\vec{E}|t \ . \qquad (27)$$

Equations 26 and 27, which are exact in the limit in which $|p_i(0)| \rightarrow 0$, demonstrate rigorously the effect that was mentioned in the discussion of Equations 15 and 16. Beginning from the situation in which all of the d's that occupy IBS's are in the lowest energy, $p_i(0) = 0$ state, when $\vec{B}$ is parallel to $\vec{E}$, $p_i(t) = \hbar k_i(t) = e/\vec{E}/t$ increases monotonically as t increases in a manner that mimics Equation 7. For this reason, in the collision-less limit it is possible for $p_i(t)$ to increase simultaneously in N_{cell} unit cells, leading to a situation in which a fusion reaction can be triggered when the common value of $k_i(t)$ approaches the boundary of the FBZ in each unit cell. In the situation in which $\vec{B}$ is perpendicular to $\vec{E}$ (as in Equation 26, with q=e), this cannot take place.

In the most general situation, $\vec{B}$ and $\vec{E}$ are neither parallel nor perpendicular to each other. In this case, with each infinitesimal change in time, $\vec{B}$ still induces changes in $p_i(t)$ that are perpendicular to it. As opposed to the situation associated with the case in which either Equation 15 or 16 is valid, the more general relationship involving Equation 14 applies, which leads to a generalization of Equation 16:

$$\hat{B} \bullet p_i(t) = \hat{B}_{\|} \bullet p_i(0) + \hat{B} \bullet \vec{E} t \ . \qquad (28)$$

Also in this case, a circular motion is induced in a quantity associated with the time evolution of $p_i(t)$, as opposed to the situation associated with either Equation 20 or 21 where it involves the time derivative (Equation 20) or the value (Equation 21) of one of its components. The quantity that follows a circular trajectory involves the second derivative of the all of the components of $p_i(t)$:

$$\frac{d^2 p_i(t)}{dt^2} = \frac{d^2 p_i(0)}{dt^2} \cos(\omega_c t) + \frac{d^2 p_i(0)}{dt^2} \times \hat{B}_{\perp} \sin(\omega_c t) \ . \qquad (29)$$

It is possible to find a solution for $p_i(t)$ by integrating Equation 29 twice and by using Equations 18 and 28. The result is:

$$p_i(t) = p_i(0) + q\vec{E} \bullet \hat{B}\hat{B}t + (-q\vec{E} \bullet \hat{B}\hat{B}t + q\vec{E} + \omega_c p_i(0) \times \hat{B}) \frac{\sin(\omega_c t)}{\omega_c}$$
$$+ (q\vec{E} \times \hat{B} - \omega_c p_i(0) + \omega_c p_i(0) \bullet \hat{B}\hat{B}) \frac{1-\cos(\omega_c t)}{\omega_c} \ . \qquad (30)$$

In the rigorous limit associated with Equations 26 and 27, in which all of the d's that are in IBS's initially occupy the lowest IBS and have vanishing wave-vector, from Equation 30 it follows that the magnitude of $p_i(t)$ is given by

$$|p_i(t)| = \sqrt{e^2 |\vec{E} \bullet \hat{B}|^2 t^2 + 4e^2 |\vec{E} \times \hat{B}|^2 \frac{\sin^2(\omega_c t/2)}{\omega_c^2}} \ . \qquad (31)$$

Thus, in the most general situation, a residual effect is present associated with the unbounded growth that occurs in $|p_i(t)|$ with increasing time when $\vec{E}$ is parallel to $\vec{B}$, through the term that involves the $|\vec{E} \bullet \hat{B}|^2$ dependence in Equation 31. The second term in the expression exhibits the same bounded behavior that occurs in the situation in which $\vec{E}$ is parallel to $\vec{B}$. As a consequence, it follows that as in the situation in which $\vec{E}$ is perpendicular to $\vec{B}$, $|p_i(t)|$ increases monotonically, as t increases without bound, provided $\vec{E}$ has a component that is parallel to $\vec{B}$. For this reason, as in the situation associated with Equation 27, in the "collision-less" limit it is possible for $p_i(t)$ to increase simultaneously in N_{cell} unit cells, leading to the triggering effect in which a fusion reaction is allowed to occur as the common value of $k_i(t)$ approaches the boundary of the FBZ in every unit cell.

SUGGESTIONS FOR ADDITIONAL EXPERIMENTS

Because the triggering effect is most pronounced when $\vec{B}$ is parallel $\vec{E}$, this may be the optimal orientation for creating excess heat. But once fusion occurs, as we discussed earlier, it is important that the ^{4}He, which is created in IBS form in the bulk, be expelled from the solid in as order-preserving fashion as possible. For this reason, it is not entirely clear that orienting $\vec{B}$ and $\vec{E}$ in this way is actually optimal.

In particular, in order to minimize the possibility that the associated effects disrupt periodic order, it seems plausible to require that the governing equation (Equation 5) associated with charge conduction be applied in an optimal way to eliminate the ^{4}He. This approach is appropriate because the conduction model that was used to explain how nuclear triggering can occur can also be used to explain how ^{4}He ions that are in IBS's can be expelled without creating disorder. The only modification that is needed to do this is to use a model for the lowest energy ion band band state that involves a different effective mass, $M^{^4\mathrm{He}}_{eff}$. In order to eliminate the ^{4}He, it also follows that because $\vec{B}$ creates an environment in which the associated fusion reactions occur with greater probability along paths that are perpendicular to $\vec{B}$, the most effective conduction processes would appear to be within planes that are also perpendicular to $\vec{B}$.

However, when $\vec{B}$ and $\vec{E}$ are parallel to each other, the current that is associated with each IBS is proportional to the group velocity $v_g(p_{\|}^{perp}) = p_{\|}^{perp}/M^{^4\mathrm{He}}_{eff}$, where the time evolution of $p_{\|}^{perp}$ is described by Equation 21, with a cyclotron angular frequency $\omega_c^{^4\mathrm{He}} = 2eB/M^{^4\mathrm{He}}_{eff}$. (Here, the convention has been adopted that in the original Equation 21, the cyclotron angular frequency ω_c is derived using the notation in which M_{eff} refers to the effective mass that applies to the band structure associated with d's that occupy the band, and that $M_{eff} \approx M^{^4\mathrm{He}}_{eff}/2$.) But as opposed to the kind of situation that occurs in the more general case (associated with Equation 30), as a function of time, the magnitude of $p_{\|}^{perp}$ remains constant and does not depend on either $\vec{B}$ or $\vec{E}$. As a consequence, when $\vec{B}$ and $\vec{E}$ are parallel to each other, in the most coherent situation in which collisions are minimized, it is conceivable that since in this limit the wave-vector of a ^{4}He that is created could be vanishingly small, the group velocity $v_g(p_{\|}^{perp})$ could also become vanishingly small. Hence, the process of expelling the ^{4}He in IBS form by conduction would be inhibited.

On the other hand, if $\vec{B}$ has components that are both parallel and perpendicular to $\vec{E}$, $p_i(t)$ has components that are perpendicular to $\vec{B}$ that are proportional to $4e\vec{E} \times \hat{B}/\omega_c$ and $4e(\vec{E} \times \hat{B}) \times \hat{B}/\omega_c$ that can be appreciable. In particular, when $\vec{B}$ and $\vec{E}$ have a relative angle of 45°, using the values $e|\vec{E}| \sim 1$eV/cm and $\omega_c \sim 2.39$ MHz (that applies for the value of $\vec{B}$ = 500 G in Letts' experiment, and when $M^{^4\mathrm{He}}_{eff}$ is approximately equal to the mass of a ^{4}He nucleus), the total magnitude of these two components is $\sim 4e|\vec{E} \times \hat{B}|/(\hbar\,\omega_c) \sim 6.77|G_i|$,

where G_i is one of the reciprocal primitive vectors(as in the situation associated with Equation 7). As a consequence, when $\vec{B}$ and $\vec{E}$ are oriented in this way, the $\vec{E}$-field induces changes in the magnitudes of the components of $p_i(t)$ to become sufficiently large in the planes that are perpendicular to $\vec{B}$ to ensure that the ^{4}He that is created there can be expelled in IBS form through Equation 5 in an optimal way.

Although each ^{4}He nucleus that is created in IBS form in the bulk could have vanishing wave-vector, the limit where this occurs (if it occurs) would involve the most coherent, collision-less situation. For this reason, as in the situation associated with the triggering process, this case probably only has relevance for establishing an idealized limit that applies for establishing a lower bound for reaction rate. It also may be relevant in situations involving smaller, nm scale crystals where it probably is desirable for collisions to be stifled. In larger crystals, collisions will occur, and the orientation in which $\vec{B}$ and $\vec{E}$ are parallel to each other, which appears to be optimal for triggering the reaction, may also be optimal for expelling each ^{4}He nucleus.

In this last kind of situation, in the presence of collisions, ^{4}He nuclei can be created in IBS form with any wave-vector. If a greater proportion of ^{4}He nuclei are created in directions that are perpendicular to $\vec{B}$, in the presence of collisions greater coupling between the ^{4}He and electromagnetic processes (including processes that involve phonons and lattice excitations) that are directed in planes that are perpendicular to $\vec{B}$ will occur. For this reason, in order to minimize energy, beginning from the most coherent limit when collisions are present in the bulk, it is plausible that the lowest lying excitations automatically will be coupled preferentially to ^{4}He in IBS's through processes that induce motion in directions that are perpendicular to $\vec{B}$. When the $\vec{B}$- and $\vec{E}$-fields are parallel, each value of the quasi-momentum $p_{\parallel}^{perp}(t)$ has a constant magnitude (as in Equation 21) but evolves in a manner that is independent of $\vec{E}$ (while it rotates at a rate that is set by the cyclotron angular frequency ω_c). Then, it may be possible to "fine tune" the excess heat process in an optimal way by increasing or decreasing ω_c (by changing the magnitude of $\vec{B}$) when this orientation is used.

It would be useful to conduct additional experiments that address either this last question and/or involve a detailed investigation of the effect of changes in the relative angle between $\vec{E}$- and $\vec{B}$-fields on excess heat. Because of the importance of expelling ^{4}He from the bulk, and the fact that this potentially could be optimized through processes that induce coupling in directions that are perpendicular to $\vec{B}$, it may be useful to introduce additional fields that accomplish this. Such experiments might involve orienting the $\vec{E}$ and $\vec{B}$ in such a way that they are parallel to each other, while introducing an additional $\vec{E}$-field in a direction that is perpendicular to them. A second possibility involves introducing ultra-sound (in place of the additional $\vec{E}$-field) in a direction that is perpendicular to the $\vec{E}$- and $\vec{B}$-fields.

Finally, assuming that the underlying framework associated with the effects of the $\vec{E}$- and $\vec{B}$-fields on the conduction of ^{4}He and d's in IBS's can explain how excess heat can be produced, it is plausible to assume that, as in the situation associated with conventional conduction (especially in situations involving smaller crystals) variations in the shapes of the crystals and their orientation with respect to each other may play a significant role in inducing excess heat. This may be playing a role in some of the observations by Swartz[36] about the importance of shape in initiating excess heat in nm scale systems.

Acknowledgment

Scott Chubb is grateful to the New Energy Foundation for support of this work. We also acknowledge valuable conversations with Mitchell Swartz.

References

1. Pons, S., Fleischmann, M. and Hawkins, M. 1989. "Electrochemically Induced Nuclear Fusion of Deuterium," *J. Electroanal. Chem.*, 261, 301.

2. Storms, E. 2007. *The Science of Low Energy Nuclear Reaction*, World Scientific.

3. Miles, M. *et al.* 1993. "Correlation of Excess Power and Helium Production During D_2O and H_2O Electrolysis Using Palladium Cathodes," *J. Electroanal. Chem.*, 346, 99-117.

4. Apicella, M.L. *et al.* 2004. "Some Recent Results at ENEA," *Proc. 11th International Conference on Cold Fusion*, Marseille, France.

5. Cravens, D. and Letts, D. 2008. "The Enabling Criteria of Electrochemical Heat: Beyond Reasonable Doubt," (in press) *Proc. 14th International Conference on Condensed Matter Nuclear Science*, Washington, D.C.

6. Bockris, J. *et al.* 1994. "Triggering of Heat and Sub-Surface Changes in Pd-D Systems," *Proc. 4th International Conference on Cold Fusion*, Lahaina, Maui, Electric Power Research Institute.

7. Cravens, D. 1993. "Factors Affecting Success Rate of Heat Generation in CF Cells," *Proc. 4th International Conference on Cold Fusion*, Lahaina, Maui, Electric Power Research Institute.

8. Letts, D. and Cravens, D. 2003. "Laser Stimulation of Deuterated Palladium: Past and Present," *Proc. 10th International Conference on Cold Fusion*, Cambridge, MA.

9. Letts, D. and Hagelstein, P.L. "Stimulation of Optical Phonons in Deuterated Palladium," (in press) *Proc. 14th International Conference on Condensed Matter Nuclear Science*, Washington, D.C.

10. Miles, M.H. Personal communication.

11. Chubb, S.R. 2005. "Nuts and Bolts of the Ion Band State Theory," *Condensed Matter Nuclear Science, Proc. 10th International Conference on Cold Fusion*, World Scientific, 735, http://www.lenr-canr.org/acrobat/ChubbSRnutsandbol.pdf

12. Puska, M.J. *et al.* 1983. "Quantum Motion of Chemisorbed Hydrogen on Ni Surfaces," *Phys. Rev. Lett.*, 51, 1081.

13. Astaldi, C. *et al.* 1992. "Vibrational Spectra of Atomic H and D on Cu(110): Evidence for H Quantum Delocalization," *Phys. Rev. Lett.*, 68, 90.

14. Nieminen, R. 1992. "Hydrogen Atoms Band Together," *Nature*, 356, 289.

15. Casella, R.C. 1983. "Theory of Excitation Bands of Hydrogen in bcc Metals and of Their Observation by Neutron Scattering," *Phys. Rev. B*, 27, 5943.

16. Chubb, S.R. "Role of Broken Gauge Symmetry in Transport Phenomena Involving Neutral and Charged Particles in Finite Lattices," http://arxiv.org/abs/cond-mat/0512363v1.

17. Chubb, S.R. and Chubb, T.A. 1990. Naval Research Laboratory MR 6600, http://newenergytimes.com/v2/library/1990/1990ChubbS-NRLReport6600.pdf

18. Chubb, T.A. and S.R. Chubb, S.R. 1990. Naval Research Laboratory MR 6617, http://newenergytimes.com/v2/library/1990/1990ChubbT-NRLReport6617.pdf

19. Chubb, T.A. and Chubb, S.R. 1990. "Bloch-Symmetric Fusion in PdD," *Fusion Technol.*, 17, 710.

20. Bush, B.F., Lagowski, J.J., Miles, M.H. and Ostrom, G.S. 1991. "Helium Production During the Electrolysis of D_2O in Cold Fusion Experiments," *J. Electroanal. Chem.*, 304, 271; Miles, M.H., Hollins, R.A., Bush, B.F., Lagowski, J.J. and Miles, R.E. 1993. "Correlation of Excess Power and Helium Production During D_2O and H_2O Electrolysis Using Palladium Cathodes," *J. Electroanal. Chem.*, 346, 99, http://www.lenr-canr.org/acrobat/MilesMcorrelatio.pdf

21. Miles, M.H., Bush, B.F. and Lagowski, J.J. 1994. "Anomalous Effects Involving Excess Power, Radiation and Helium Production During D_2O

Electrolysis Using Palladium Cathodes," *Fusion Technol*., 25, 478; Miles, M.H., Bush, B.F. and Johnson, K.B. 1996. "Anomalous Effects in Deuterated Systems," NAWCWPNS TP 8302, Naval Air Warfare Weapons Division, http://www.lenr-canr.org/acrobat/MilesManomalousea.pdf

22. McKubre, M.C.H., Crouch-Baker, S., Riley, A.M., Smedley, S.I. and Tanzella, F.L. 1993. "Excess Power Observations in Electrochemical Studies of the D/Pd System: The Influence of Loading," *Proc. 3rd International Conference on Cold Fusion, Frontiers of Cold Fusion*, Universal Academy Press, 5, http://www.lenr-canr.org/acrobat/McKubreMCHexcesspowe.pdf

23. Hagelstein, P.L., McKubre, M.C.H., Nagel, D.J., Chubb, T.A. and Hekman, R.J. 2005. "New Physical Effects in Metal Deuterides," *Condensed Matter Nuclear Science, Proc. 11th International Conference on Cold Fusion*, World Scientific, 23, http://www.lenr-canr.org/acrobat/Hagelsteinnewphysica.pdf

24. Chubb, S.R. and Chubb, T.A. 2010. "Potential Role of Ion Band States in Nuclear Fusion in Finite Solids," submitted to *Phys. Rev. Lett.*, 2010; Chubb, T.A. and Chubb, S.R. 2009. "Overcoming the Coulomb Barrier in Cold Fusion," *J. Condensed Matter Nucl. Sci*., 2, 1–9, http://www.cfescience.com/yahoo_site_admin/assets/docs/pdfCoulBar.80171500.pdf

25. McKubre, M.C.H. *et al*. 1995. "Concerning Reproducibility of Excess Power Production," *Proc. ICCF5*, 17, http://lenr-canr.org/acrobat/PonsSproceeding.

26. Ashcroft, N.W. and Mermin, N.D. 1976. *Solid State Physics*, Saunders College Publishing, 64-82, http://en.wikipedia.org/wiki/Crystal_momentum

27. *Ibid*., http://en.wikipedia.org/wiki/Reciprocal_lattice

28. *Ibid*., http://en.wikipedia.org/wiki/Brillouin_zone

29. Bloch, F. 1928. "Über die Quantenmechanik der Elektronen in Kristallgittern," *Z. Phys*., 52, 555.

30. Zener, C. 1934. "A Theory of the Electrical Breakdown of Solid Dielectrics," *Proc. R. Soc. A*, 145, 855, 523.

31. Feldmann, J. *et al*. 1992. "Optical Investigation of Bloch Oscillations in a Semiconductor Superlattice," *Phys. Rev. B*, 46, 7252.

32. Dahan, M.B. *et al*. 1996. "Bloch Oscillations of Atoms in an Optical Potential," *Phys. Rev. Lett*., 76, 4508; Wilkinson, S.R. *et al*. 1996. "Observation of Atomic Wannier-Stark Ladders in an Accelerating Optical Potential," *Phys. Rev. Lett*., 76, 4512.

33. Chubb, S.R. 2006. *Condensed Matter Nuclear Science, Proc. 11th International Conference on Cold Fusion*, World Scientific, 646, http://www.lenr-canr.org/acrobat/ChubbSRframeworkf.pdf. Note the following correction: $i_1\Delta t_1=i_2\Delta t_2=4\pi N_{vert}/a|eE|=t_{trig}=3.03$ μs, on the final page, should be replaced with the expression, $i_1\Delta t_1=i_2\Delta t_2=4\pi N_{vert}^3\hbar/a|eE|=t_{trig}=0.68$ *ms*.

34. Chubb, S.R. 2005. *Condensed Matter Nuclear Science, Proc. 12th International Conference on Cold Fusion*, World Scientific, 430, http://www.lenr-canr.org/acrobat/ChubbSRcontextfor.pdf. Note the correction provided to Ref. 33 (last citation) and the following corrections to the final page of this reference: The original text, "Crystals that…6nm, which have tunneling times~microseconds," should be replaced by," Crystals that…6nm, which have tunneling times~milliseconds;" and the original text, "Crystals…~60nm will create heat…(~3 ms)," should be replaced by, "Crystals…~60nm will create heat…(~3 s)."

35. *Op. cit*. ref. 26, http://en.wikipedia.org/wiki/Reciprocal_lattice

36. Chubb, S. and Dolan, T. 2010. "Summary of the 2010 Colloquium on Lattice-Assisted Nuclear Reactions at MIT," *Infinite Energy*, 16, 93, 16, http://www.infinite-energy.com/images/pdfs/Colloquium2010.pdf

About the Authors

Dr. Scott Chubb was employed as a research physicist at the Naval Research Laboratory (NRL) between 1989 and 2009. Prior to joining NRL, he worked there as a contractor for SFA, Inc. (1988-1989), and as a National Research Council fellow (1985-1988). He began his career as a research associate at Northwestern University (1982-1985). An author of more than 60 technical papers, he has been an editor of numerous cold fusion publications and participated in the ten-year study, sponsored by the Office of Naval Research, that documented the existence of cold fusion heat (associated with the work of Fleischmann and Pons).

Dennis Letts has been working on electrochemical heat systems since 1990. He has built over 600 cells to study deuterium in palladium systems. He has pioneered the use of radio frequencies and lasers to trigger exothermic events in D-Pd electrochemical cells.

*Email: chubbscott@aol.com
**Email: lettslab@sbcglobal.net